Approximating Hydropower Systems by Feasibility Spaces in Stochastic Dual Dynamic Programming

Arild Helseth
SINTEF Energy Research
Trondheim, Norway
arild.helseth@sintef.no

***Abstract*—This work investigates and improves methodology for approximating hydropower systems by feasibility spaces, which can be embedded in the stochastic dual dynamic programming algorithm and applied in the context long-term hydrothermal scheduling. The feasibility spaces are derived from optimization of the detailed hydropower system and are expressed in few dimensions to facilitate efficient computations. Test results from a case study for the Norwegian power system demonstrate how feasibility spaces serve to realistically constrain the hydropower system.**

***Index Terms*—Power generation scheduling, hydroelcetric power generation, optimization methods, stochastic processes.**

I. Introduction

Long-term scheduling (LTS) of hydropower storages is an important task in hydro-dominated power systems which is typically accommodated in a single computer model with a planning horizon of multiple years. LTS models are important in toolchains for operational planning [1], and are frequently used for planning tasks, such as system analyses [2], expansion planning [3], and maintenance planning [4]. As LTS models are normally not used for detailed system dispatch, the need for technical details in such models constitutes a trade-off between accuracy of results and computation time. On the one hand, explicit treatment of physical reservoirs, plants, and waterways in hydro-dominated systems may lead to excessive computation times. On the other, system simplifications in LTS models could lead to time-inconsistent policies [5], revealing a need for embedding more details from the short-term scheduling into LTS models [6].

A variety of methodologies have been proposed for solving the LTS problem, and the use of methods based on optimization has matured over the last decades [7]. In particular the stochastic dual dynamic programming (SDDP) algorithm introduced in [8] has been widely applied in operative scheduling models [9], [10], and is subject to improvements and extensions by the research community [11]–[13].

Equivalent representations (ER) of the reservoirs and plants in a system or an area is a commonly used technique to reduce dimensionality and computation time in hydrothermal scheduling models [9], [10], [14]–[18]. The use of ERs, where the sum of potential energy in the reservoirs is represented rather than the water in each reservoir, was introduced in [19], and is often found to be a reasonable approximation for systems with large regulation capability and hydrologically homogenous basins [20]. In general terms, ER parameters are fitted so that the simulated results of the equivalent system are similar to those obtained from the detailed system. As discussed in [21], and later demonstrated in [22], local constraints on reservoirs, flows and generations seen in the detailed system are difficult to account for in aggregated models, possibly leading to suboptimal use of hydropower resources. Moreover, ER parameters are typically estimated prior to running the LTS optimization models, and the parameter state-dependencies cannot be easily accounted for.

A different technique was presented in [23], constraining decisions related to the aggregated hydropower system by *feasibility spaces* defined by linear inequalities (or *cuts*). These linear inequalities can be directly derived from optimization of the detailed hydropower system. The feasibility spaces were embedded in the SDDP algorithm in [23], where aggregated reservoir volumes and inflows constitute the state variables. The state-dependency was accounted for, allowing feasibility spaces to be shared between different states within a given decision stage in the SDDP algorithm. A similar methodology is presented in [24], where low-dimensional hydropower surfaces are computed for complex power plants based on a optimization of the detailed hydropower system. Differently from [24], the feasibility spaces in [23] represent cascaded systems and are demonstrated in a context of a stochastic scheduling model.

Being a direct derivation from optimization of the detailed system, and with a well-defined state-dependency that can be accounted for in LTS algorithms such as SDDP, the feasibility spaces are worthwhile further exploration. In this work the SDDP algorithm is applied to an aggregated representation of the Norwegian hydropower system which is constrained by feasibility spaces. The work in [23] is extended in two ways. First, the dimensionality of the feasibility space is significantly reduced to improve computational performance. Second, the method is demonstrated on a representation of the Norwegian power system. Consequently, this work contributes to further develop and verify the application of feasibility spaces within

Submitted to the 23rd Power Systems Computation Conference (PSCC 2024). This work was funded by The Research Council of Norway Project No. 344220

the SDDP algorithm for the purpose of striking a better balance between hydropower system representation and computation time in LTS models.

The paper is outlined as follows. First, the overall problem is described followed by a detailed mathematical formulation of the decomposed stage-wise decision problem in Section II. Subsequently, the process of creating feasibility spaces is elaborated in Section III. Computational experiments with the presented model are presented in Section IV, before concluding in Section V.

II. Problem Description

A. Problem Formulation and Decomposition

The LTS optimization problem can be defined as in (1), where x_t are the state variables y_t the stage variables for each decision stage t. One seeks an operating strategy minimizing the expected cost of supplying electricity in (1a), while accounting for the end-of-horizon valuation of stored water in $\Psi(x_T)$, and respecting constraints in (1b)-(1d). A planning horizon of multiple years is assumed, with weekly decision stages, and with a finer time discretization, referred to as time steps, within the week. The stage variables represent the operational decisions to be made in each stage and time step, while state variables transfer information about the system state between stages.

$$\min_{(x_1,y_1),\ldots,(x_T,y_T)} \mathbb{E}\left\{ \sum_{t=1}^{T} f_t(x_t,y_t) + \Psi(x_T) \right\} \tag{1a}$$

$$\text{s.t.} \quad \mathbf{W}x_t + \mathbf{H}x_{t-1} + \mathbf{G}y_t = h(\xi_t) \tag{1b}$$

$$\mathbf{B}y_t = 0 \tag{1c}$$

$$(x_t, y_t) \in X_t \tag{1d}$$

$$\forall t \in \{1, 2, \ldots, T\}$$

The constraints are indicated in (1b)-(1d), where the initial state vector x_0 is given, X_t is the feasible set for the decision variables of decision stage t, and $\mathbf{W}$, $\mathbf{H}$, $\mathbf{G}$, and $\mathbf{B}$, are matrices of suitable dimensions. The expectation in (1a) is taken over the stochastic inflow. Inflow to the EERs is represented by a vector autoregressive model of first order according to the procedure described in [25]. The right-hand-side parameter vector $h(\xi_t)$ in (1b) is dependent on the random vector of inflow "white noise" ξ_t whose distribution is known, and where ξ_t are the realizations. Although the focus is on uncertainty in inflow in this work, other uncertainties such as wind power and electricity demand can in principle be included in the autoregressive model and treated within the SDDP algorithm. Examples of joint treatment of inflow and wind power uncertainty within SDDP can be found in [26].

The problem in (1) can be classified as a multi-stage stochastic optimization problem, which may be efficiently solved by decomposition techniques [27]. This work applies the SDDP algorithm, which is a sampling-based variant of multi-stage Benders decomposition. The problem in (1) can be decomposed into stage-wise nested linear programming (LP) problems of type:

$$\mathcal{Q}_t(x_{t-1}) = \min_{x_t, y_t} f_t(x_t, y_t) + \alpha_t(x_t) \tag{2a}$$

$$\text{s.t.} \quad (x_t, y_t) \in X_t(x_{t-1}, \xi_t) \tag{2b}$$

In short, the SDDP algorithm consists of forward and backward iterations, repeatedly solving stage-wise decision problems of type (2). The variable α_t expresses the future expected cost seen from the end of stage t. This variable will gradually be constrained by Benders cuts constructed in the SDDP backward iterations. The SDDP forward iterations provide simulated state space trajectories corresponding to a set of sampled inflow scenarios.

In Section II-B we elaborate on the stage-wise decision problem in (2), while the creation of feasibility spaces is described in Section III.

B. Stage-wise Decision Problem

The decision problem for a *decision stage* t with *time steps* $k \in \mathcal{K}$ is defined as an LP problem in (3), detailing the general formulation in (2). The system is grouped into price areas $a \in \mathcal{A}$ which are simply referred to as *areas* in the following. It is assumed that decisions related to hydropower describe an aggregated response per area, with no grid bottlenecks within the area. In the formulation below hourly time steps are assumed without explicit conversion between energy and power, to ease presentation. Note that some technical constraints, such as ramping constraints, may need a finer time resolution to meet their intended purpose. Variable units are either in €(α), MWh $(p^H, p^G, p^D, p^R, q^S, r, v, I, f)$, or MW (c).

$$\mathcal{Q}_t(\mathbf{v}^*_{t-1}, \mathbf{z}_{t-1}) = \min \sum_{k\in\mathcal{K}} \sum_{a\in\mathcal{A}} \Bigg[\sum_{g\in\mathcal{G}_a} C^G_{gt} p^G_{gtk} - \sum_{d\in\mathcal{D}_a} C^D_{dt} p^D_{dtk} + C^R p^R_{atk} \Bigg] + \alpha_t \tag{3a}$$

$$\mathbf{v}_{t-1} = \mathbf{v}^*_{t-1} \qquad : \boldsymbol{\pi}^v \tag{3b}$$

$$\mathbf{z}_t = \boldsymbol{\Phi}\mathbf{z}_{t-1} + \boldsymbol{\epsilon}_t \qquad : \boldsymbol{\pi}^z \tag{3c}$$

$$I_{at} = \sigma_{at} z_{at} + \mu_{at} \qquad \forall a \tag{3d}$$

$$v_{at} + \sum_{k\in\mathcal{K}} p^H_{atk} + q^S_{at} - v_{a,t-1} - I_{at} = 0 \qquad \forall a \tag{3e}$$

$$p^H_{atk} + \sum_{g\in\mathcal{G}_a} p^G_{gtk} - \sum_{d\in\mathcal{D}_a} p^D_{dtk} + p^R_{atk} + \sum_{\ell\in\mathcal{L}^+_a} f_{\ell tk} - \sum_{\ell\in\mathcal{L}^-_a} f_{\ell tk} \geq D_{atk} - W_{atk} \qquad \forall a, k \tag{3f}$$

$$\sum_{a\in\mathcal{A}} c^H_{at} \geq R \tag{3g}$$

$$p^H_{atk} - c^H_{at} \geq \underline{P}^H_{at} \qquad \forall a, k \tag{3h}$$

$$p^H_{atk} + c^H_{at} \leq \overline{P}^H_{at} \qquad \forall a, k \tag{3i}$$

$$p^H_{atk} - p^H_{at,k-1} - r_{at} \leq 0 \qquad \forall a, k \tag{3j}$$

$$p^H_{at,k-1} - p^H_{at,k} - r_{at} \leq 0 \qquad \forall a,k \quad (3k)$$

$$\alpha_t + \sum_{a\in\mathcal{A}} \pi^v_{act} v_{at} + \sum_{a\in\mathcal{A}} \pi^z_{act} z_{at} \geq \beta^B_{ct} \qquad \forall c \quad (3l)$$

$$\gamma^v v_{at} + \gamma^e e^H_{at} + \gamma^r r_{at} + \gamma^c c^H_{at} + \kappa^v v_{a,t-1} + \kappa^i I_t \leq \beta^F_{act} \qquad \forall a,c \quad (3m)$$

$$e^H_{at} - \sum_{k\in\mathcal{K}} p^H_{atk} = 0 \qquad \forall a \quad (3n)$$

$$0 \leq p^G_{gtk} \leq \overline{P}^G_{gt} \qquad \forall g,k \quad (3o)$$

$$0 \leq p^D_{dtk} \leq \overline{P}^D_{dt} \qquad \forall d,k \quad (3p)$$

$$\underline{V}_{at} \leq v_{at} \leq \overline{V}_{at} \qquad \forall a \quad (3q)$$

$$-\overline{F}_{\ell t} \leq f_{\ell tk} \leq \overline{F}_{\ell t} \qquad \forall \ell,k \quad (3r)$$

The vectors of energy volumes ($\mathbf{v}^*_{t-1} = \left[v^*_{a,t-1}, \forall a\right]$) and normalized inflows ($\mathbf{z}_{t-1} = \left[z^*_{a,t-1}, \forall a\right]$) from the previous stage are considered state variables, so that $x_t = \left[\mathbf{v}^*_{t-1}, \mathbf{z}_{t-1}\right]$. The objective in (3a) seeks to minimize the costs associated with operation of the system in the current decision stage and the expected cost of operating system in the future. The current cost comes from thermal generation (p^G) at marginal cost C^G and curtailment of price-inelastic demand (p^R) at marginal cost C^R, while the coverage of price-elastic demand (p^D) is seen as a revenue with marginal value C^D. The sets $\mathcal{G}_a$ and $\mathcal{D}_a$ comprise the thermal generators and price-elastic demands in area a, respectively. The future expected cost is represented by α_t which is constrained by Benders cuts in (3l).

In (3b) a copy of the reservoir volume state variables are taken, for the ease of finding their dual values $\boldsymbol{\pi}^v$. The weekly normalized inflow ($\mathbf{z}_t = [z_{at}, \forall a]$) to each area is described in (3c), as a vector autoregressive model of first order. The correlation matrix ($\boldsymbol{\Phi}$) and residuals ($\boldsymbol{\epsilon}_t$) are fitted to observations, where residuals are adapted to a three-parameter lognormal distribution according to [25], and where the normalized inflow is converted to energy inflow (I_{at}) by using the standard deviation (σ_{at}) and mean (μ_{at}) in (3d).

Hydro energy storage balances per area are provided in (3e), where the energy storage (v_{at}) is balanced against hydropower generation (p^H), spillage (q^S), initial storage, and inflow. An energy balance for each price area and time step is defined in (3f), allowing exchange of energy (f_ℓ) between connected areas to $\mathcal{L}^+_a$ and from $\mathcal{L}^-_a$ area a. Price-inelastic demand (D) and wind power (W) are treated as parameters in the energy balances.

A reserve capacity requirement (R) for the system is included in (3g), where reserved capacity per area (c^H_{at}) is accounted for in generation limits of the area in (3h) and (3i). As a simplification, it is assumed that i) the hydropower system should cover the reserve requirement R alone, ii) that the area contributions are constant over the week and symmetric with respect to up- and down-regulation capacity, and that iii) reserves can be exchanged across the system without grid bottlenecks.

In (3j) and (3k) a maximum allowed ramping rate (r_{at}) limits the ability to change hydropower generation upwards and downwards between time steps, respectively. Note that the ramping rate is a decision variable that enters the feasibility cuts, as described in Section III.

Benders cuts in (3l) are constructed in the backward iteration of the SDDP algorithm and comprise elements from cut coefficient vectors $\boldsymbol{\pi}^v$, $\boldsymbol{\pi}^z$, and $\boldsymbol{\beta}^B$, where $\boldsymbol{\pi}^v$ and $\boldsymbol{\pi}^z$ are extracted as dual values from (3b) and (3c), respectively.

Feasibility cuts in (3m) constrain decisions related to the hydropower system for a specific area, and are expressed in the dimensions of end volume (v_t), sum energy production (e^H), maximum allowed ramping rate (r), reserve capacity (c^H), initial storage (v_{t-1}), and inflow (I), and where $\boldsymbol{\gamma}$, $\boldsymbol{\kappa}$, and $\boldsymbol{\beta}^F$ denote the feasibility cut coefficients. The derivation of feasibility cuts is further described in Section III. Note that (3n) defined the auxiliary variable e^H to ease the formulation in (3m). Variable boundaries are presented in (3o)-(3r).

III. Feasibility Spaces

Ideally, the detailed hydropower system should be considered explicitly in the problem formulation in Section II-B. For large-scale hydropower systems this typically involves several hundreds of storages with separate time series for inflow, substantially increasing the state space to be considered in the SDDP algorithm. Instead, a spatial decomposition technique is applied where the system problem in (3) is viewed as the master problem providing the aggregate hydropower schedule per area, and where a set of detailed hydropower problems per area of type (4) are the subproblems in which the feasibility of aggregated schedules is tested. The subproblems are formulated as LP problems under the assumption that hydropower operational costs can be neglected. In this setup, details in the hydropower system are coordinated between the master and subproblems through feasibility cuts which, under conditions elaborated in [23], may provide an exact approximation of the detailed hydropower system.

The feasibility cuts in (3m) coordinate aggregate hydropower decisions (x_t, y_t) provided the initial state x_{t-1} with a detailed system description, as illustrated in Fig. 1 and described below. In (3), the operation of the hydropower system for each area a is represented by four variables: stored energy at the end of the decision period (v_{at}), energy production (e^H_{at}), maximum allowed ramping (r_{at}), and reserved capacity (c^H_{at}). State variable decisions are classified as $x_t = \{v_{at}\}$, stage variable decisions as $y_t = \{e^H_{at}, r_{at}, c^H_{at}\}$, and initial states as $x_{t-1} = \{v_{a,t-1}, I_t\}$.

The detailed hydropower problem per area a and decision stage t is formulated as in (4), where $\mathbf{A}$, $\mathbf{M}$, $\mathbf{C}_x$, $\mathbf{C}_y$, and $\mathbf{E}$ are matrices of suitable dimensions.

$$\min_{(x^d_{at}, u_{at})} \sum u_{at} \qquad (4a)$$

$$\text{s.t.} \quad \mathbf{A}x^d_{at} + \mathbf{M}x^*_{a,t-1} = 0 \qquad : \boldsymbol{\kappa} \quad (4b)$$

$$\mathbf{A}'x^d_{at} + \mathbf{C}_x x^*_{at} + \mathbf{C}_y y^*_{at} + \mathbf{E}u_{at} = 0 \qquad : \boldsymbol{\gamma} \quad (4c)$$

The objective is to minimize constraint violations in (4c) expressed by a vector of slack variables u_{at}. The matrix $\mathbf{A}$

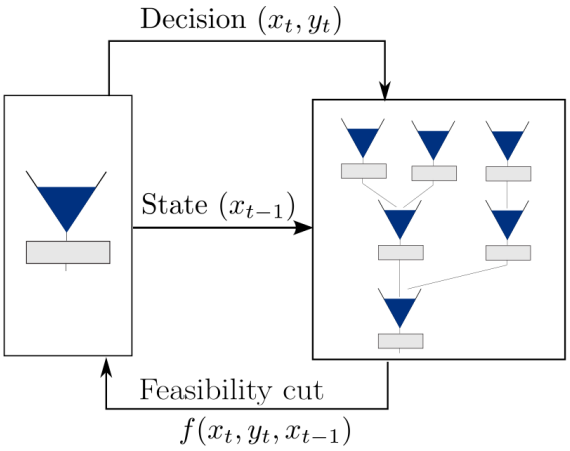

Fig. 1: Illustration of the process for creating feasibility cuts.

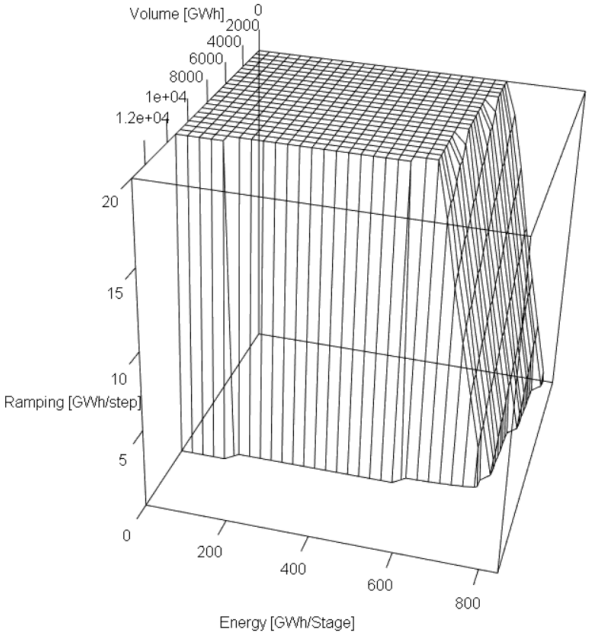

Fig. 2: Feasibility space for area 4 in week 1 for case presented in Section IV.

and decision variables x^d_{at} represent the basic constraints of the detailed system. The creation of feasibility cuts follows three steps:

1) Disaggregate decisions. The initial state $x^*_{a,t-1}$ is distributed to the corresponding detailed hydropower problem defined in (4). This involves mapping the initial energy storage and sum energy inflow to the detailed reservoirs. The matrix $\mathbf{M}$ in (4b) provides this mapping. Note that to preserve convexity of the SDDP algorithm, the mapping cannot be state-dependent. In this work a time dependent mapping was used, distributing energy inflow and initial energy storage to the individual reservoirs according to their relative shares of average inflow and energy storage capability, respectively.

2) Define requirements. The hydropower stage (y^*_{at}) and state (x^*_{at}) decisions obtained from the solution of (3) define requirements in (4c), formulated as linear inequalities with slack variables u_{at}. Trial schedules of stored energy (v^*_{at}), energy production (e^{H*}_{at}), maximum allowed ramping (r^*_{at}), and reserved capacity (c^{H*}_{at}) provide the requirements in (4c).

3) Check for feasibility. If the requirements defined in (4c) are all met, the trial decisions are feasible. If not, at least one of the dual values (γ) of constraints (4c) is nonzero, and a feasibility cut of type (3m) is created.

Step 2) above differs from [23] in that the sum energy for the whole decision period (e^{H*}_{at}) rather than the energy produced per time step (p^{H*}_{at}) is formulated as a requirement. Thus, the number of constraints in (4c) and, consequently, the dimensionality of the feasibility cut is reduced. For studies with many time steps within each decision stage, a large number of feasibility cuts were needed with the approach in [23] to adequately approximate the high-dimensional feasibility space. This became a bottleneck for large-scale systems. With the formulation in (3m), the dimensionality of the feasibility cut does not depend on the number of time steps, and thus the computational burden is significantly reduced when solving (3) with many time steps. The maximum allowed ramping rate supplements the sum-energy requirement, testing the ramping capability of the detailed hydropower system. Assumptions regarding the frequency of this requirement in (4c) are needed since decisions per time step are not communicated to (4). In this study the detailed hydropower system was required to ramp up and down to meet r^*_{at} once per day.

As elaborated in [23], feasibility cuts can be created either prior to running SDDP or as an integral part of the SDDP algorithm. In this work, feasibility cuts were computed beforehand for each area. Each of the stage and state variables were discretized in 5 values according to their extremal values, and (4) was solved for each possible combination to obtain feasibility cuts, according to the three steps described above. Redundant and numerically similar cuts were removed.

Finally, a set of feasibility cuts of type (3m) was obtained for each area. These cut sets can be seen as state-dependent feasibility spaces for each area. For visualization of such spaces, one can discretize cut variables and find the binding cut for each combination of discrete variables. This was done for area 4 in the case study presented in Section IV, as illustrated in Fig. 2. As documented in Table I, area 4 has 63 reservoirs with at least 10 Mm^3 storage capacity and 53 power stations with at least 10 MW installed capacity. Fig. 2 spans the dimensions volume (v), sum energy (e^H), and ramping (r). The initial reservoir level, inflow, and reserve capacity requirements were fixed to take average values. A feasible combination of v, e^H, r should be within the surface in Fig. 2. As seen from Fig. 2, the maximum possible storage at the end of the decision period decreases both with increasing energy production and with increasing ramping rate.

IV. Computational Experiments

A. Case Description

The SDDP algorithm with aggregated hydropower description and with feasibility cuts was implemented in `Julia`,

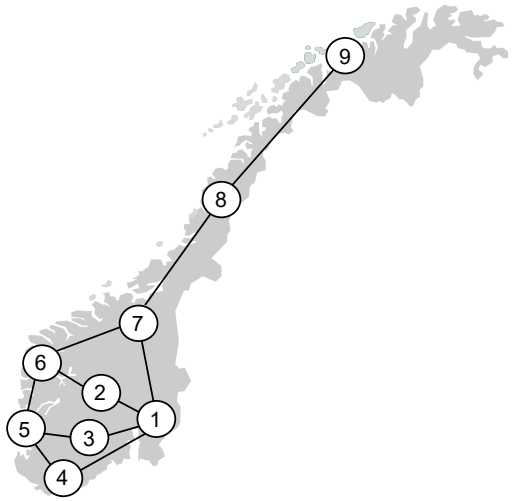

Fig. 3: Area topology for the Norwegian power system.

using the `JuMP` package [28], solving LP problems with CPLEX version 20.1. The computational tests reported were conducted on an Intel Core i7-9850H processor with maximum frequency of 4.60 GHz and 64 GB RAM, allowing 7 parallel worker processes in both the forward and backward iterations.

Computational tests were carried out on a description of the Norwegian power system. The system description includes possible future expansions towards 2030, but excludes existing connections to the surrounding European power system, treating Norway as an isolated system. The system comprises 9 areas, connected together as shown in Fig. 3. Characteristics of the detailed hydropower systems within each area are provided in Table I, listing the number of reservoirs (N_r) and power plants (N_p) exceeding defined limits. Many of the physical reservoirs and power stations are part of complex hydropower cascades, and each area comprise multiple cascades. The hydropower system accounts for more than 35 GW installed capacity and 92 TWh storage capacity and has an average annual inflow of 152 TWh. Hydropower is supplemented by approximately 9.5 GW thermal generation capacity and 7.0 GW of installed wind power capacity to serve the demand. The computational experiments are conducted on a realistic representation of the Norwegian hydropower system balanced with fictitious demand and supply from other technologies. The reduced system size allowed demonstration of the proposed methodology on a large-scale hydropower system while keeping computation times at a reasonable level. Note that a wider system boundary, e.g, including Northern Europe, is possible without modifications of the proposed methodology.

A scheduling horizon of 3 years was applied with weekly decision stages and with 42 4-hour time steps within each week. The statistical model for energy inflow was derived based on data from 126 inflow time series considering a period of 30 years (1961-1990) with weekly inflow measurements. The SDDP model was run with 70 inflow scenarios in each forward SDDP iteration, and 7 discrete inflow white noise terms were sampled at each stage in the backward SDDP

TABLE I: Hydropower per area.

Area	$N_r \geq$ **10 Mm**^{3}	$N_p \geq$ **10 MW**	$\overline{V}$ **[TWh]**	$\overline{p}^H$ **[GW]**
1	30	36	3.85	2.94
2	50	52	9.87	3.24
3	26	25	8.91	2.31
4	63	53	13.16	5.02
5	34	31	13.98	4.18
6	69	53	13.20	7.17
7	108	92	10.30	5.00
8	34	24	11.54	2.80
9	47	31	7.79	2.40
Sum	461	397	92.60	35.06

iterations. Consequently, a total of $70 \times 156 = 10920$ decision problems of type (3) were solved in the forward iteration and $70 \times 7 \times 156 = 76440$ in the backward iteration. A maximum number of 80 SDDP iterations was applied in the experiments. Feasibility cuts were created prior to the SDDP run, as described in Section III, providing between 50-130 feasibility cuts per area and decision stage. Advanced cut management for treatment of Benders and feasibility cuts was not considered.

The SDDP model was run for two cases: A **Base** case with no feasibility cuts, and a **Feas**ibility case where feasibility cuts of type (3m) were included. This resulted in different *strategies* in terms of Benders cuts of type (3l) for each case. These strategies were used in two different simulations: An **Aggregate** simulation using sampled energy inflow scenarios according to (3c) together with the model formulation in (3), and a **Detailed** simulation using detailed historical inflow observations and a detailed description of the hydropower system, as applied in (4), embedded in (3).

B. Simulation Results – Aggregate

After computing Benders cuts of type (3l), a final forward simulation was conducted for each of the Base and Feas cases with 2000 separately sampled inflow scenarios. Since the operation of the hydropower system is more constrained in case Feas than in case Base, the cost of operation is higher in the former. Fig. 4 shows that the simulated power prices, found as the dual values of (3f), for area 1 are significantly higher in case Feas than in case Base. The price spikes around weeks 20 and 70 indicate a tight power balance around the beginning of the snow melting period.

The duration curves for hydropower generation for areas 6 and 7 are shown in Fig. 5. Utilization of the maximum generation capacity in case Feas is clearly lower than in Base, shifting more generation at lower output. Furthermore, time series of changes in generation are presented as duration curves in Fig. 6, indicating the limited ramping capability in case Feas compared to Base.

C. Simulation Results – Detailed

The detailed hydropower system was simulated using historical observations from 30 historical inflow years (1961-1990) and with the strategies from the Base and Feas cases. In these simulations, the stage problem consisted of the problem

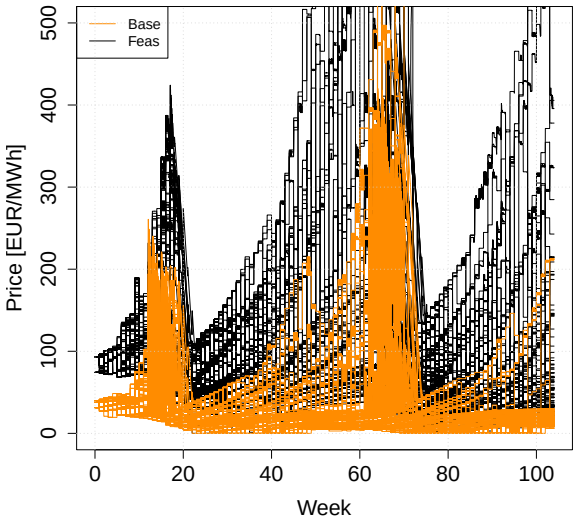

Fig. 4: Simulated power prices for cases Base and Feas.

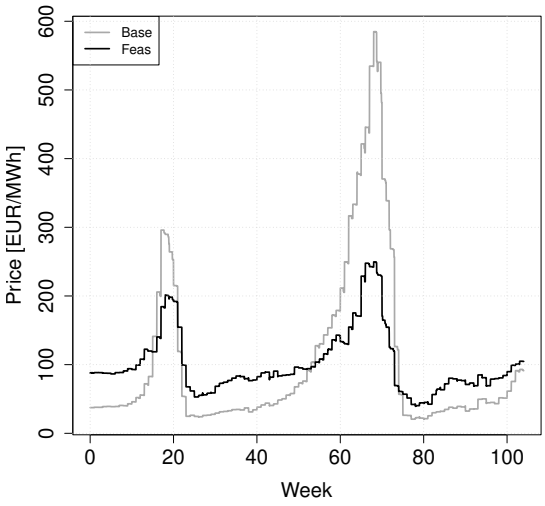

Fig. 7: Average power prices for cases Base and Feas.

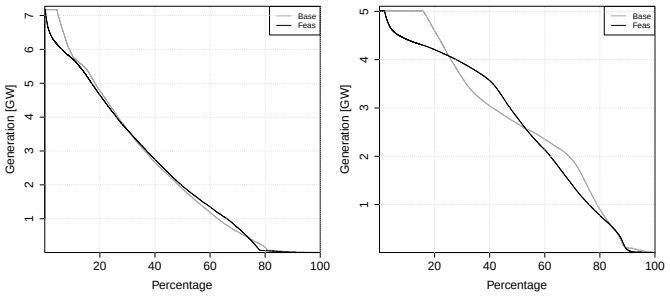

Fig. 5: Duration curves for generation for areas 6 (left) and 7 (right).

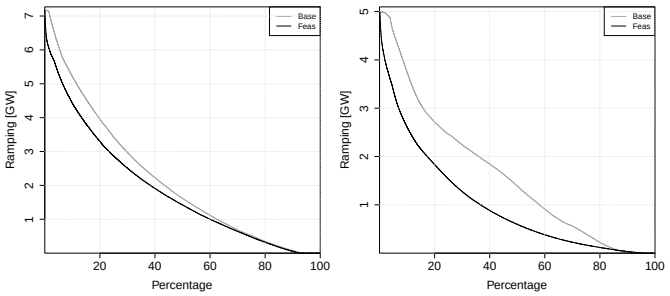

Fig. 6: Duration curves for changes in generation (ramping) for areas 6 (left) and 7 (right).

defined in Section II, but with a detailed description of the hydropower system including historical inflow time series associated with each physical reservoir. Years were arranged in 30 sequences to be simulated, defining 1961-1963 as the first sequence, 1962-1964 the second, and so on.

Results from these detailed simulations are not always as one expects, since the simulated system differs from the aggregated system that was used when computing SDDP strategies. While one in the simulation considers inflows to physical reservoirs, the strategies are computed based on a statistical model for inflow per area. Moreover, the feasibility cuts used in case Feas were computed assuming a fixed and balanced mapping of aggregate initial reservoir and inflow to the detailed system (step 1 in Section III), and thus do not capture the true variability in the detailed system. Still, detailed simulations on historical data are important as they serve to validate the new methodology on the problem that motivated its creation.

The total cost for a simulated sequence was found as $\sum_{t=1,..,T}\Big(\mathcal{Q}_t - \alpha_t\Big)$, where $\mathcal{Q}_t$ is expressed in (3a). In addition, the difference in stored water at the end of horizon was accounted for according to a common reference value. The total cost of operating the system was lower in 21 out of 30 simulated sequences, and was on average 7.2 % lower when following the Feas rather than the Base strategy.

The average simulated power prices for all areas and simulated scenarios for the two first years are shown in Fig. 7. The prices obtained following the Feas strategy are more stable than for the Base strategy, with lower price spikes when the power balance is particularly tight around weeks 18 and 70.

The simulated operation of detailed hydropower reservoirs provide an indication of how well the aggregated strategies in cases Base and Feas reflect the hydropower details. In Fig. 8, simulated trajectories for the large reservoir Svartisen, located in area 8, are shown. Although the simulated operation of

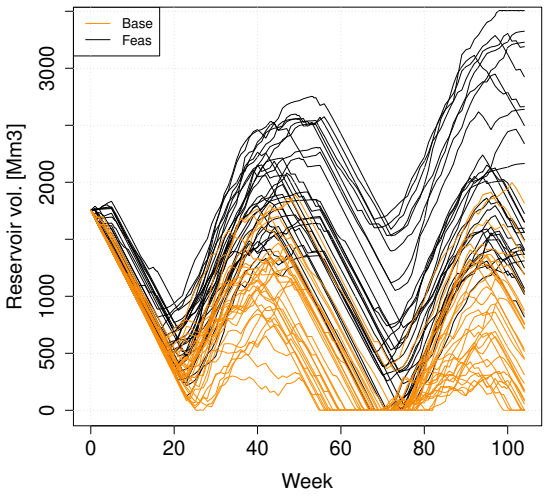

Fig. 8: Reservoir trajectories for Svartisen for cases Base and Feas.

the majority of individual reservoirs are more balanced in the Feas case, similar to what we observe in Fig. 8, there are many examples where the Feas case provides poor reservoir handling as well.

D. Computational Performance

Running the SDDP model with the problem setup and technical specifications defined in Section IV-A took 10.7 and 27.6 hours for cases Base and Feas, respectively. Thus, including feasibility cuts in case Feas increases computation time with a factor of 2.7. As a comparison, results from [23] [Table 1, cases REF and STAT-FC] on a much smaller data set and with a higher-dimensional feasibility cuts, indicate a ratio of 8.7 (Case REF took 370 seconds while case STAT-FC took 3204 seconds.).

For the Feas case, a stage LP problem of type (3) comprises around 10k variables and 4k constraints, out of which approximately 25% are feasibility cuts. As a comparison, when simulating with detailed hydropower, the stage LP problem comprises 350k variables and 158k constraints. Such problem sizes would lead to prohibitive computation times if solved within the SDDP algorithm using the parameterization defined in Section IV-A.

Note that the computation time for case Feas depends on the discretization when creating feasibility cuts. Some experiments with different discretizations were conducted, revealing that finer discretization did not improve result quality significantly, and that coarser discretization tends to compromise result quality.

V. Conclusion

This work presents a computationally efficient approximation of hydropower systems by feasibility spaces which can be embedded within the SDDP algorithm and applied to the long-term hydrothermal scheduling problem. The feasibility spaces can be derived based on optimization of the detailed hydropower system prior to running SDDP, and their state-dependency can be accounted for.

Simulation results based on SDDP strategies with and without feasibility spaces were compared, demonstrating how these spaces constrain hydropower operation. A simulation explicitly including the detailed hydropower system indicated better resource utilization when following SDDP strategies based on feasibility spaces.

References

[1] A. Helseth, A. C. G. Melo, Q. M. Ploussard, B. Mo, M. E. P. Maceira, A. Botterud, and N. Voisin, "Hydropower Scheduling Toolchains: Comparing Experiences in Brazil, Norway, and USA and Implications for Synergistic Research," *Journal of Water Resources Planning and Management*, vol. 149, no. 7, 2023.

[2] A. Philpott and Z. Guan, "Models for estimating the performance of electricity markets with hydro-electric reservoir storage," University of Auckland, New Zealand, Tech. Rep., 2013.

[3] S. Jaehnert, O. Wolfgang, H. Farahmand, S. Völler, and D. Huertas-Hernando, "Transmission expansion planning in Northern Europe in 2030 - Methodology and analyses," *Energy Policy*, vol. 61, pp. 125–139, 2013.

[4] R. M. Chabar, S. Granville, M. V. F. Pereira, and N. A. Iliadis, *Optimization of Fuel Contract Management and Maintenance Scheduling for Thermal Plants in Hydro-based Power Systems*, ser. Energy, Natural Resources and Environmental Economics. Springer, Berlin, Heidelberg, 2010, ch. 13, pp. 201–219.

[5] A. W. Rosemberg, A. Street, J. D. Garcia, D. Valladão, T. Silva, and O. Dowson, "Assessing the cost of network simplifications in long-term hydrothermal dispatch planning models," *IEEE Transactions on Sustainable Energy*, vol. 13, no. 1, pp. 196–206, 2021.

[6] L. Bernardinelli and L. S. A. Martins, "Equilibrium approach to the single solution of longer- and shorter-term hydro-thermal scheduling problems," in *6th International Conference on Clean Electrical Power*, Santa Margherita Ligure, Italy, 2017.

[7] A. R. de Queiroz, "Stochastic hydro-thermal scheduling optimization: An overview," *Renewable and Sustainable Energy Reviews*, vol. 62, pp. 382–395, 2016.

[8] M. V. F. Pereira and L. M. V. G. Pinto, "Multi-stage stochastic optimization applied to energy planning," *Mathematical Programming*, vol. 52, pp. 359–375, 1991.

[9] A. Gjelsvik, B. Mo, and A. Haugstad, *Handbook of Power Systems I*. Springer, 2010, ch. Long- and medium-term operations planning and stochastic modelling in hydro-dominated power systems based on stochastic dual dynamic programming, pp. 33–55.

[10] M. Maceira, D. Penna, A. Diniz, R. Pinto, A. Melo, C. Vasconcellos, and C. Cruz, "Twenty Years of Application of Stochastic Dual Dynamic Programming in Official and Agent Studies in Brazil – Main Features and Improvements on the NEWAVE Model," in *Proc. 20th Power System Computation Conference*, 2018.

[11] A. Papavasiliou, Y. Mou, L. Cambier, and D. Scieur, "Application of Stochastic Dual Dynamic Programming to the Real-Time Dispatch of Storage Under Renewable Supply Uncertainty," *IEEE Transactions on Sustainable Energy*, vol. 9, no. 2, pp. 547–558, 2018.

[12] M. N. Hjelmeland, J. Zou, A. Helseth, and S. Ahmed, "Nonconvex medium-term hydropower scheduling by stochastic dual dynamic integer programming," *IEEE Transactions on Sustainable Energy*, vol. 10, no. 1, pp. 481–490, 2018.

[13] A. L. Diniz, M. E. P. Maceira, C. L. V. Vasconcellos, and D. D. J. Penna, "A combined SDDP/Benders decomposition approach witha risk-averse surface concept for reservoir operation in long-term power generation planning," *Annals of Operations Research*, vol. 292, pp. 649–681, 2020.

[14] O. J. Botnen, A. Johannesen, A. Haugstad, S. Kroken, and O. Frøystein, "Modelling of hydropower scheduling in a national/international context," in *Hydropower 92*, E. Brock and D. Lysne, Eds., Lillehammer, 1992.

[15] L. Söder and J. Rendelius, "Two-Station Equivalent of Hydropower Systems," in *Power System Computation Conference*, Liege, Belgium, 2005.

[16] M. E. P. Maceira, V. S. Duarte, D. D. J. Penna, and M. P. Tcheou, "An approach to consider hydraulic coupled systems in the construction of equivalent reservoir model in hydrothermal operation planning," in *Power System Computation Conference (PSCC)*, Stockholm, Sweden, 2011.
[17] E. Blom, L. Söder, and D. Risberg, "Performance of multi-scenario equivalent hydropower models," *Electric Power Systems Research*, vol. 187, 2020.
[18] V. L. de Matos and E. C. Finardi, "A computational study of a stochastic optimization model for long term hydrothermal scheduling," *International Journal of Electrical Power and Energy Systems*, vol. 43, no. 1, pp. 1443–1452, 2012.
[19] N. V. Arvanitidis and J. Rosing, "Composite Representation of a Multireservoir Hydroelectric Power System," *IEEE Transactions on Power Apparatus and Systems*, vol. 89, no. 2, pp. 319–326, 1970.
[20] M. V. F. Pereira and L. M. V. G. Pinto, "Stochastic optimization of a multireservoir hydroelectric system: A decomposition approach," *Water Resources Research*, vol. 21, no. 6, pp. 779–792, 1985.
[21] V. R. Sherkat, R. Campo, K. Moslehi, and E. O. Lo, "Stochastic Long-Term Hydrothermal Optimization for a Multireservoir System," *IEEE Transactions on Power Apparatus and Systems*, vol. 104, no. 8, pp. 2040–2050, 1985.
[22] J. L. Brandao, "Performance of the Equivalent Reservoir Modelling Technique for Multi-Reservoir Hydropower Systems," *Water Resources Management*, vol. 24, pp. 3101–3114, 2010.
[23] A. Helseth and B. Mo, "Hydropower Aggregation by Spatial Decomposition—An SDDP Approach," *IEEE Transactions on Sustainable Energy*, vol. 14, no. 1, pp. 381–392, 2023.
[24] Q. Ploussard, T. D. Veselka, K. Oikonomou, and N. Voisin, "Hydro-economics tradeoff surfaces to guide unit commitment in production cost models," *Applied Energy*, vol. 324, no. 119728, 2022.
[25] M. E. P. Maceira and C. V. Bezerra, "Stochastic Streamflow Model for Hydroelectric Systems," in *Proc. 5th conf. on Probabilistic Methods Applied to Power Systems*, 1997.
[26] M. E. P. Maceira, A. C. G. Melo, J. F. M. Pessanha, C. B. Cruz, V. A. Almeida, and T. C. Justino, "Combining monthly wind and inflow uncertainties in the stochastic dual dynamic programming – Application to the Brazilian interconnected system," *Energy Systems*, 2023.
[27] J. R. Birge and F. Louveaux, *Introduction to Stochastic Programming*, 2nd ed. Springer, 2011.
[28] I. Dunning, J. Huchette, and M. Lubin, "JuMP: A modeling language for mathematical optimization," *SIAM Review*, vol. 59, no. 2, pp. 295–320, 2017.